Reorganization of corticostriatal circuits in healthy G2019S *LRRK2* carriers

Rick C. Helmich, MD, PhD*
Avner Thaler, MD*
Bart F.L. van Nuenen, MD, PhD
Tanya Gurevich, MD
Anat Mirelman, PhD
Karen S. Marder, MD, MPH
Susan Bressman, MD
Avi Orr-Urtreger, MD, PhD
Nir Giladi, MD
Bastiaan R. Bloem, MD, PhD
Ivan Toni, PhD
On behalf of the LRRK2 Ashkenazi Jewish Consortium

ABSTRACT

Objective: We investigated system-level corticostriatal changes in a human model of premotor Parkinson disease (PD), i.e., healthy carriers of the G2019S *LRRK2* mutation that is associated with a markedly increased, age-dependent risk of developing PD.

Methods: We compared 37 asymptomatic *LRRK2* G2019S mutation carriers (age range 30–78 years) with 32 matched, asymptomatic nonmutation carriers (age range 30–74 years). Using fMRI, we tested the hypothesis that corticostriatal connectivity in premotor PD shifts from severely affected to less affected striatal subregions, as shown previously in symptomatic PD. Specifically, we predicted that in premotor PD, the shift in corticostriatal connectivity would follow the same gradient of striatal dopamine depletion known from overt PD, with the dorsoposterior putamen being more affected than the ventroanterior putamen.

Results: The known parallel topology of corticostriatal loops was preserved in each group, but the topography of putamen connectivity shifted. In *LRRK2* G2019S mutation carriers, the right inferior parietal cortex had reduced functional connectivity with the dorsoposterior putamen but increased connectivity with the ventroanterior putamen, as compared with noncarriers. This shift in functional connectivity increased with age in *LRRK2* G2019S mutation carriers.

Conclusions: Asymptomatic *LRRK2* G2019S mutation carriers show a reorganization of corticostriatal circuits that mirrors findings in idiopathic PD. These changes may reflect premotor basal ganglia dysfunction or circuit-level compensatory changes. ***Neurology*® 2015;84:399–406**

Correspondence to Dr. Helmich: rick.helmich@radboudumc.nl

GLOSSARY

DAT = dopamine transporter; **FWE** = family-wise error; ***GBA*** = β-glucocerebrosidase; ***LRRK2*** = leucine-rich repeat kinase 2; **MNI** = Montreal Neurological Institute; **PD** = Parkinson disease; **ROI** = region of interest; **SMA** = supplementary motor area; **SPM** = Statistical Parametric Mapping.

Parkinson disease (PD) is a progressive, neurodegenerative disorder characterized by nigrostriatal dopamine depletion. The motor symptoms of PD appear only when dopaminergic cell death reaches a critical threshold of 50% to 80%.[1] This suggests that the nervous system has a marked potential to compensate for these changes.[2] However, human studies of cerebral compensation in premotor PD are lacking, given the difficulty of predicting who will develop PD in the future.

Previous work has shown that compensatory mechanisms in idiopathic PD depend on brain regions relatively unaffected by dopamine depletion, such as the anterior striatum.[3,4] Using fMRI in early-stage PD, we recently showed a shift in corticostriatal connectivity from severely affected striatal regions (posterior putamen) to less affected striatal regions (anterior putamen).[5] If these changes reflect compensation, they should also occur in the premotor phase of PD, when functional reorganization of cerebral circuits prevents overt clinical symptoms.[2]

Supplemental data at Neurology.org

*These authors contributed equally to this work.

From the Centre for Cognitive Neuroimaging (R.C.H., I.T.), Donders Institute for Brain, Cognition and Behaviour, Radboud University Nijmegen; Department of Neurology (R.C.H., B.R.B.), Donders Institute for Brain, Cognition and Behaviour, Radboud University Medical Center, Nijmegen, the Netherlands; Movement Disorders Unit, Department of Neurology (A.T., T.G., A.M., N.G.), and Genetic Institute (A.O.-U.), Tel Aviv Sourasky Medical Center; Sackler School of Medicine (A.T., T.G., A.O.-U., N.G.), Tel Aviv University, Israel; Department of Neurology (B.F.L.v.N.), Catharina Hospital, Eindhoven, the Netherlands; Columbia University (K.S.M.), Columbia University Medical Center, New York; and Beth Israel Medical Center (S.B.), New York, NY.

LRRK2 Ashkenazi Jewish Consortium coinvestigators are listed on the *Neurology*® Web site at Neurology.org.

Go to Neurology.org for full disclosures. Funding information and disclosures deemed relevant by the authors, if any, are provided at the end of the article.

We tested this prediction in a genetic model of premotor PD, comparing corticostriatal functional connectivity between healthy carriers and noncarriers of the G2019S mutation in the *LRRK2* gene. *LRRK2* parkinsonism is associated with Lewy body pathology[6] and with similar clinical signs as idiopathic PD.[7,8] Healthy carriers of the *LRRK2* G2019S mutation therefore form a unique population at risk of PD.[9,10] Penetrance estimations range from 10%–17% at the age 50 years to 25%–85% at the age of 70 years,[7,11–13] suggesting that the risk of developing PD is age-dependent.[7] Thus, we investigated age-related changes in corticostriatal connectivity in healthy *LRRK2* G2019S mutation carriers.

METHODS

Subjects. We recruited 75 healthy first-degree relatives of leucine-rich repeat kinase 2 (*LRRK2*) Ashkenazi Jewish patients with PD into this study through their affected PD family members. All patients with PD were recruited from the Movement Disorder Unit of Tel Aviv Sourasky Medical Center, as part of a larger study (the Michael J. Fox Ashkenazi Jewish LRRK2 Consortium) aimed to characterize the G2019S mutation phenotype. Participants were not aware of their genetic status throughout the study. Exclusion criteria were clinical diagnosis of PD according to the Queen Square Brain Bank criteria, the presence of a mutation in the β-glucocerebrosidase (*GBA*) gene (an independent risk factor for developing PD[14]), other neuropsychiatric diseases, and general exclusion criteria for MRI scanning (e.g., claustrophobia, pacemaker, implanted metal parts). Of 75 tested subjects, 6 were excluded. Reasons for exclusion were a panic attack in the MRI scanner (n = 1), technical problems (storage failure; n = 2), and the presence of a *GBA* mutation (n = 3). Of 69 included subjects, 37 (20 women) were carriers of the *LRRK2* G2019S mutation and 32 (16 women) were noncarriers. The 69 subjects came from 43 families, 18 of which had ≥2 included subjects (range 2–5 members, average ± standard error = 2.4 ± 0.86 members).

Standard protocol approvals, registrations, and patient consents. Before the beginning of the study, all subjects signed an informed consent form approved by Tel Aviv Sourasky Medical Center institutional review board. Genomic DNA was isolated from peripheral blood leukocytes, and the 6055G_A (G2019S) mutation in exon 41 of the *LRRK2* gene was determined as previously described.[14] All subjects were administered the Unified Parkinson's Disease Rating Scale, Part III, the Beck Depression Inventory II, the State-Trait Anxiety Inventory, and the University of Pennsylvania Smell Identification Test. We compared *LRRK2* G2019S mutation carriers and noncarriers using 2-sample *t* tests.

Image acquisition. During scanning, all subjects were asked to keep their eyes closed and to avoid repetitive thoughts. Imaging was performed on a GE 3T Signa HDxt scanner (GE Signa EXCITE, Milwaukee, WI) with a resonant gradient echoplanar imaging system, using a standard 8-channel head coil. Each subject received an anatomical scan (spoiled gradient echo sequence: field of view 250 × 250 mm; matrix size 256 × 256 mm; voxel size 0.98 × 0.98 × 1 mm; repetition time = 9 milliseconds; echo time = 3.6 milliseconds) and 266 functional scans (single-shot gradient echoplanar imaging sequence: echo time/repetition time = 35/1,680 milliseconds; 30 axial slices; voxel size = 3.1 × 3.1 × 3.5 mm; no gap; scanning time approximately 7.5 minutes; 266 images).

Preprocessing of imaging data. Data were preprocessed and analyzed with SPM5 (Statistical Parametric Mapping, www.fil.ion.ucl.ac.uk/spm). Images were spatially realigned, slice-time corrected, normalized to Montreal Neurological Institute (MNI) space using unified segmentation, and smoothed with an isotropic 8-mm full width at half maximum gaussian kernel. We then low-pass filtered the images using a fifth-order Butterworth filter to retain frequencies below 0.1 Hz, because correlations between intrinsic fluctuations are specifically found in this frequency range.[15] Anatomical images were spatially coregistered to the mean of the functional image and spatially normalized using the same transformation matrix applied to the functional images.

Striatal seed regions. We segmented each subject's normalized anatomical MRI scan into left and right putamen, caudate nucleus, and nucleus accumbens (using FIRST v1.1; www.fmrib.ox.ac.uk/fsl). We further subdivided the putamen into a dorsoposterior part, a ventroposterior part, a dorsoanterior part, and a ventroanterior part using the y = 0 and z = 0 axes as the borders between the 4 subregions.[16] Finally, we averaged across the left and right striatal regions because none of the subjects had asymmetric signs of PD. We used MarsBaR (http://marsbar.sourceforge.net) to calculate the average BOLD time courses of the bilateral dorsoposterior putamen, ventroposterior putamen, dorsoanterior putamen, ventroposterior putamen, caudate nucleus, and accumbens (figure 1).

Nuisance signals. We removed nonneuronal fluctuations from the data by adding 3 time courses to our model that describe the average signal intensity in the bilateral lateral ventricles (CSF), a blank portion of the MRIs (out-of-brain signal), and the global gray matter signal. To optimally control for the motion effects, we added 36 motion parameters to our model, as described before.[17]

Statistical analyses. ***First-level analyses.*** For each subject, we performed a multiple regression analysis using the general linear model implemented in SPM. This model included the time courses of the 6 striatal seed regions and the 39 nuisance regressors. All regressors and functional images were bandpass-filtered between 0.008 and 0.l Hz. Parameter estimates (β values) for all regressors were obtained by maximum-likelihood estimation, modeling temporal autocorrelation as an AR(1) process. For each seed region, the parameter estimate reflects the influence of the seed region's time course on the time course of that voxel, while controlling for the contribution of all the other regressors in the model.[18] Thus, common variance (e.g., global signal fluctuations) is not assigned to any of the regressors, increasing the specificity of our findings.

Second-level analyses. Group-level analyses were performed using a random-effects model implemented in SPM. For each group, we entered the β images of the 6 striatal seed regions into a 2 × 6 repeated-measures analysis of variance with the factors group (*LRRK2* G2019S mutation carriers vs noncarriers) and region (dorsoposterior putamen, ventroposterior putamen, dorsoanterior putamen, ventroposterior putamen, caudate nucleus, and accumbens). For each of the 6 regions, we investigated both common and differential connectivity between groups. Based on previous findings in idiopathic PD,[5] we focused our group comparison on a single region of interest (ROI), i.e., the right inferior parietal cortex (12-mm sphere around MNI coordinates [+56, −20, +28]). We also performed a whole-brain search. The statistical threshold was set to $p < 0.05$ family-wise error (FWE)-corrected for the search volume. Finally, we correlated corticostriatal connectivity with age for both *LRRK2* G2019S mutation carriers and noncarriers, using sex as a covariate of no interest.

Figure 1 Striatal seed regions

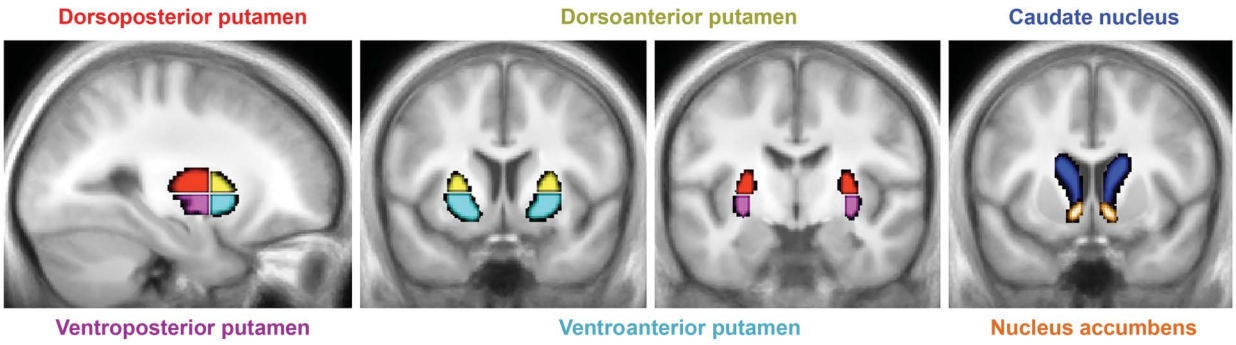

Six striatal seed regions, overlaid onto the average structural MRI of the 37 *LRRK2* G2019S mutation carriers and 32 noncarriers. The putamen is divided into 4 regions, using the lines passing through the anterior commissure (y = 0) and z = 0 (in MNI [Montreal Neurological Institute] space) as the borders, based on previous work.[16]

Voxel-based morphometry. Using the DARTEL toolbox in SPM8, we compared gray matter volume between groups. Age, sex, and total intracranial volume were added as covariates of no interest. We focused our group comparison on ROIs in the inferior parietal cortex and bilateral basal ganglia.

RESULTS *LRRK2* G2019S mutation carriers and noncarriers. *LRRK2* G2019S mutation carriers (n = 37) and noncarriers (n = 32) did not differ in age, sex, or clinical scores (table 1). On average, carriers and noncarriers moved <0.5 mm in all 3 axes during scanning (no group difference; $p > 0.5$).

Similar corticostriatal connectivity between groups. Both groups showed significant functional connectivity between each of the striatal subregions and other brain areas (tables e-1 to e-3 on the *Neurology*® Web site at Neurology.org) (figure 2). Specifically, the dorsoposterior putamen was connected to regions involved in motor execution (supplementary motor area [SMA], primary motor cortex); the ventroposterior putamen to the brainstem and cerebellum; the dorsoanterior putamen to regions involved in motor planning (pre-SMA and rostral dorsal premotor cortex; the ventroanterior putamen to temporoparietal regions; the caudate nucleus to regions involved in cognitive control (dorsolateral and dorsomedial prefrontal cortex); and the nucleus accumbens to regions involved in emotional processing (orbitofrontal cortex). The spatial distribution of these brain regions follows the known anatomy of corticostriatal loops,[19] in line with a diffusion tensor imaging study in humans,[20] previous resting-state fMRI studies,[5,21] and a meta-analysis of cortical and striatal coactivation patterns.[16]

Differential corticostriatal connectivity between groups. ***ROI analyses.*** There was a significant group (carriers > noncarriers) × striatal region (ventroanterior putamen >

Table 1 Subject characteristics

	Asymptomatic noncarriers	Asymptomatic *LRRK2* G2019S carriers	*p* Value
No.	32	37	
Age, y	46.3 ± 10.6	49.4 ± 10.5	0.22
Sex, % women	50	54	
Handedness	30 RH/2 LH	32 RH/5 LH	
UPDRS III	1.9 ± 1.6	2.1 ± 1.9	0.55
Beck Depression Inventory[a]	2.6 ± 3.1	3.4 ± 5.0	0.46
STAI-S[b]	31.3 ± 11.9	33.8 ± 11.9	0.40
STAI-T[b]	31.8 ± 10.2	35.8 ± 11.6	0.14
UPSIT[c]	31.4 ± 5.7	31.8 ± 3.4	0.71

Abbreviations: LH = left-handedness; RH = right-handedness; STAI-S = State-Trait Anxiety Inventory–state anxiety; STAI-T = State-Trait Anxiety Inventory–trait anxiety; UPDRS III = Unified Parkinson's Disease Rating Scale, Part III; UPSIT = University of Pennsylvania Smell Inventory Test.
This table summarizes the clinical characteristics (average ± SD) for the 3 groups that were measured.
[a] Data available for 30 noncarriers and 34 carriers.
[b] Data available for 30 noncarriers and 36 carriers.
[c] Data available for 29 noncarriers and 32 carriers; a higher UPSIT score indicates better olfaction.

Figure 2 Shared corticostriatal connectivity between *LRRK2* G2019S mutation carriers and noncarriers

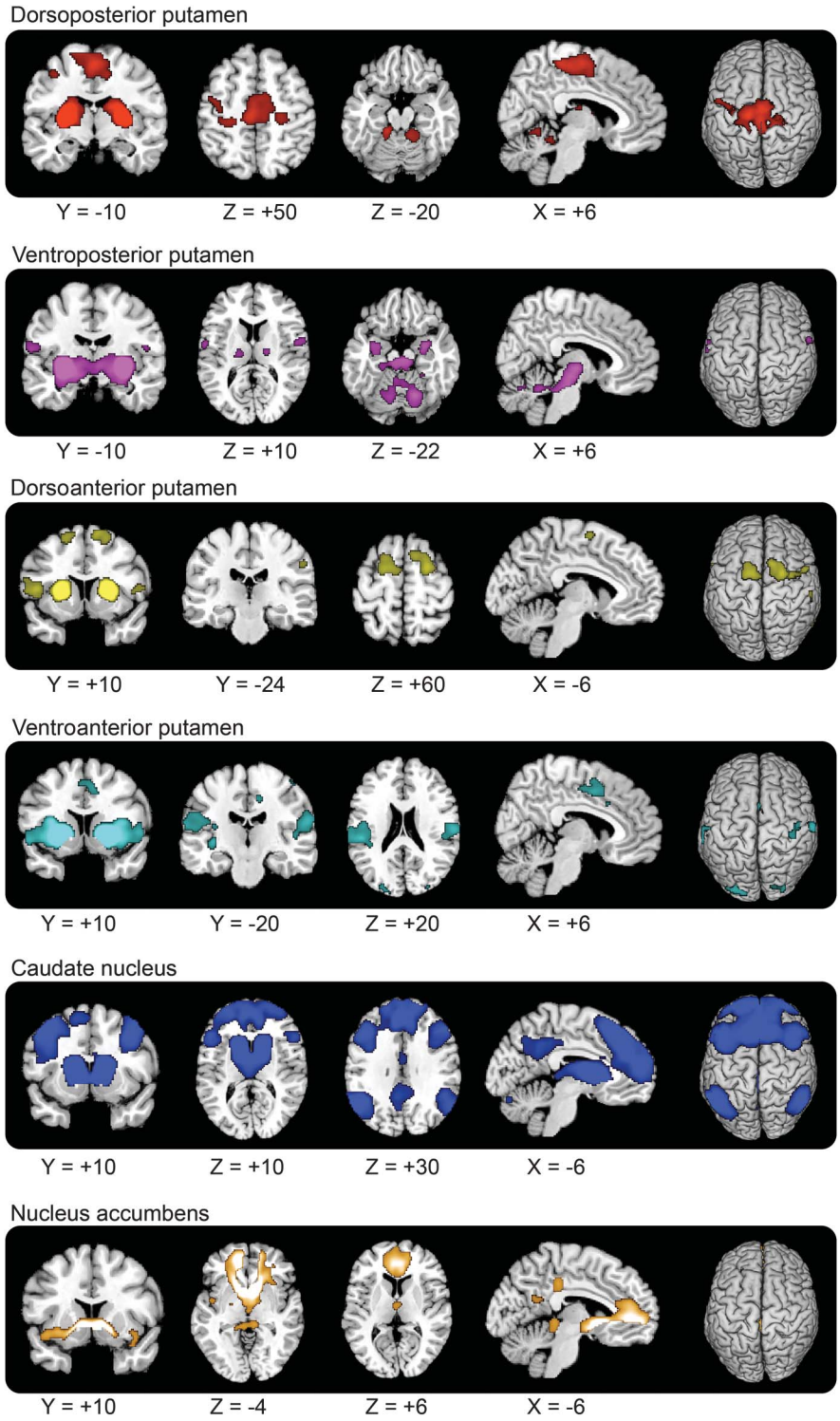

The images represent SPM{t} maps of similar functional connectivity across groups, thresholded at $p < 0.001$ uncorrected (for graphical purposes), with a cluster extent threshold of 50 voxels, overlaid on anatomical images from a representative subject of the MNI (Montreal Neurological Institute) series.

dorsoposterior putamen) interaction in the right rolandic operculum (MNI coordinates [+54, −10, +22], $p = 0.023$ FWE-corrected, $t = 3.54$) (figure 3). Anatomically, this region was assigned to OP4 (30% probability) in the right inferior parietal cortex. This finding indicates that corticostriatal connectivity of the right inferior parietal cortex was shifted from the dorsoposterior putamen to the ventroanterior putamen in *LRRK2* G2019S mutation carriers vs noncarriers. Using the equivalent ROI in the left hemisphere, we found the same

Figure 3 Differential corticostriatal connectivity between *LRRK2* G2019S mutation carriers and noncarriers

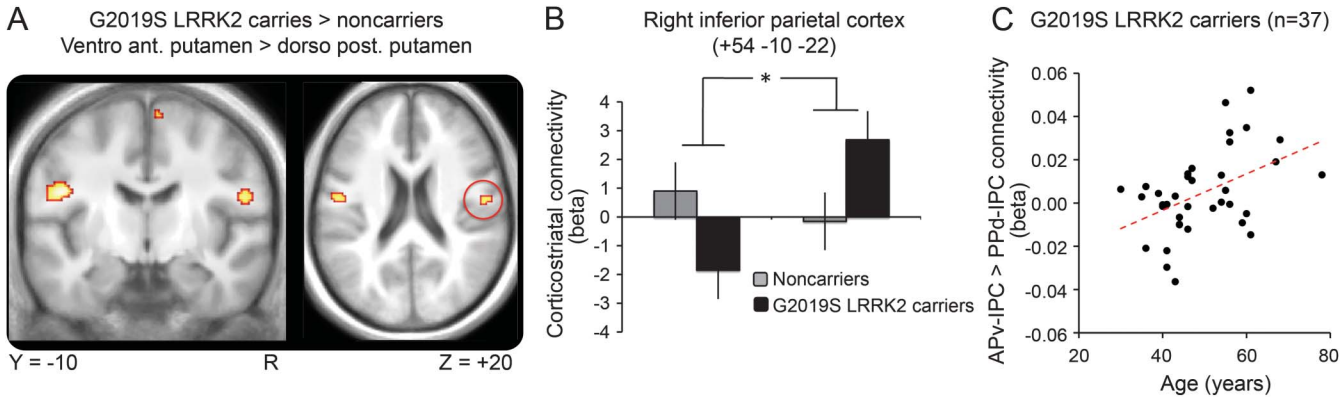

(A) SPM{t} of functional connectivity showing an interaction between group (*LRRK2* G2019S mutation carriers, noncarriers) and seed region (dorsoposterior putamen, ventroanterior putamen), overlaid onto the average MRI of all 69 subjects. For graphical purposes, the contrast is shown at a threshold of $p < 0.001$ uncorrected with a cluster extent threshold of 10 voxels. (B) Connectivity strength between the 2 seed regions of interest (dorsoposterior putamen, ventroanterior putamen) and the right IPC, separately for *LRRK2* G2019S mutation carriers (black bars) and matched noncarriers (gray bars). The y-axis indicates the β values (in SEM units) of a multiple regression analysis, averaged across subjects; that is, the unique contribution of each seed region's BOLD time series to the BOLD time series of the right IPC. Error bars indicate SEM (normalized to 1). (C) Correlation between age and the shift in corticostriatal connectivity in 37 *LRRK2* G2019S mutation carriers. On the y-axis, β values from the local maximum in the right IPC as shown in panel A (MNI coordinates: [+50, −18, +32] for the *LRRK2* G2019S mutation carriers). APv = ventroanterior putamen; BOLD = blood oxygen level dependent; IPC = inferior parietal cortex; MNI = Montreal Neurological Institute; PPd = dorsoposterior putamen.

interaction in the left inferior parietal cortex (MNI coordinates [−48, −12, +24], $p = 0.011$ FWE-corrected, $t = 3.77$). When we flipped the contrast images in the axial plane and statistically compared the strength of corticostriatal connectivity in a voxel-wise manner between both hemispheres, we observed no significant lateralization ($p > 0.5$). Post hoc separate analyses for the dorsoposterior and ventroanterior putamen did not reveal significant group differences. At a more liberal threshold of $p < 0.001$ uncorrected (cluster extent threshold of 10 voxels), we observed additional areas within the motor circuit showing a similar shift in corticostriatal connectivity (table 2).

Correlation of corticostriatal connectivity with age in *LRRK2* G2019S mutation carriers. The shift in corticostriatal connectivity (from dorsoposterior to ventroanterior putamen) of the right inferior parietal cortex (MNI coordinates [+50, −18, +32], $t = 3.63$, $p = 0.032$ FWE-corrected) increased with age in the carriers (age range 30–78 years) but not in the noncarriers (age range 30–74 years) (figure 3). The interaction between group and age was not significant ($p > 0.05$). There was no significant relationship between age and functional connectivity of other striatal subregions.

Gray matter volume. Gray matter volume in the bilateral basal ganglia or inferior parietal cortex did not differ between groups.

DISCUSSION There are 2 main findings. First, corticostriatal connectivity of the right inferior parietal cortex was shifted from the dorsoposterior to the ventroanterior putamen in *LRRK2* G2019S mutation

Table 2 Corticostriatal connectivity as a function of group (carriers, noncarriers) and striatal subregion (PPd, APv)

Functional region	Anatomical region	Hemisphere	MNI coordinates, x, y, z	t Value	p Value (uncorrected)	Cluster size, voxels
Ventroanterior putamen > dorsoposterior putamen, *LRRK2* G2019S mutation carriers > noncarriers						
Somatosensory cortex and operculum	44% in BA3a, 20% in OP4	L	−48, −8, +24	4.31	<0.001	115
	53% in BA3b, 26% in OP4, 4% in OP3	R	+54, −10, +20	3.58	<0.001	27
Anterior cingulate cortex	NA	L	−16, 0, +42	3.51	<0.001	17
Somatosensory and premotor cortex	46% in BA1, 39% in BA6	R	+50, −16, +56	3.31	<0.001	15
Precentral gyrus	NA	L	−36, +4, +44	3.49	<0.001	10
SMA	100% BA6	R	+8, −8, +68	3.38	<0.001	11
Putamen	NA	L	−22, +8, −4	3.40	<0.001	19

Abbreviations: APv = ventroanterior putamen; BA = Brodmann area; MNI = Montreal Neurological Institute; NA = not applicable; OP = operculum parietale; PPd = dorsoposterior putamen; SMA = supplementary motor area.

carriers, mirroring similar findings in idiopathic PD.[5] We observed a similar shift in corticostriatal connectivity of the left inferior parietal cortex. The latter finding should be considered with more caution because our a priori hypothesis concerned the right hemisphere.[5] Second, this shift in corticostriatal connectivity increased with age in *LRRK2* G2O19S mutation carriers but not in noncarriers. These findings show that corticostriatal connectivity shifts from more affected to less affected striatal regions in healthy subjects at risk of developing PD.

There is a wide range of reported penetrance between 25% and 100% for the *LRRK2* mutation overall.[22] For Ashkenazy Jews carrying the G2019S *LRRK2* mutation (i.e., the population tested here), lifetime penetrance until the age of 80 years has been estimated to be 26%.[13] Thus, it is striking that we found altered corticostriatal connectivity in a group of *LRRK2* G2O19S mutation carriers with an average age of ±50 years. Although the shift in corticostriatal connectivity was age-dependent, it was not driven by outliers: the cerebral effects were normally distributed over subjects (figure 3C), and removal of the 10% highest values (4 carriers) did not change the significance of the effect. Clinically healthy mutation carriers may not manifest motor symptoms because they do not develop nigrostriatal dopamine depletion, or, if they have dopamine deficiency, they may develop cerebral mechanisms that successfully compensate for nigrostriatal cell loss. Thus, the proportion of *LRRK2* G2O19S mutation carriers developing symptomatic PD (26%) may not necessarily reflect the proportion of carriers developing cerebral changes. Accordingly, we previously showed that healthy *LRRK2* G2O19S mutation carriers have task-related cerebral changes without behavioral impairments[9,10] and subtle changes in gait and cognition[23,24] without overt PD symptoms. These cerebral and behavioral markers may potentially serve to quantify cerebral dysfunction and compensatory reserve of *LRRK2* G2O19S mutation carriers, in order to predict who will develop PD in the future.

Given the dorsoposterior to ventroanterior gradient of striatal dopamine depletion in PD, dopamine depletion in the premotor phase probably starts in the posterior putamen. Evidence for premotor nigrostriatal dopamine depletion has recently been shown in a large group of asymptomatic G2019S *LRRK2* mutation carriers (aged 41–86 years), of whom 85% had abnormal substantia nigra hyperechogenicity (compared with 95% of patients with PD) and 44% had an abnormal dopamine transporter (DAT) scan. The carriers with an abnormal DAT scan were significantly older than the carriers with a normal DAT scan.[25] Another study reported that 2 of 5 asymptomatic mutation carriers from a single R1441X *LRRK2* family had abnormal DAT binding in the putamen, and one of those subjects showed a further reduction of DAT binding and subtle clinical parkinsonism a few years later.[26] A third study in 2 families with Y1699C and R1441X mutations in the *LRRK2* gene reported that 2 of 6 asymptomatic mutation carriers had abnormal DAT binding, with another 2 developing such abnormalities (but not clinical signs) over 4 years of follow-up.[27] Finally, work in G2019S *LRRK2* mice showed an age-dependent decrease in striatal dopamine content.[28] These findings indicate that a large proportion of healthy *LRRK2* G2O19S mutation carriers have ongoing nigrostriatal pathology, and that these pathologic changes increase with age. This fits with the age-dependent penetrance of the *LRRK2* mutation.[7,11,12] Based on these findings, we suggest that the age-dependent changes in corticostriatal connectivity in *LRRK2* G2O19S mutation carriers reflect underlying striatal (dopaminergic) dysfunction.

In healthy *LRRK2* G2O19S mutation carriers, corticostriatal connectivity of the inferior parietal cortex was shifted toward the ventroanterior putamen. This change may reflect compensatory adaptation, primary pathology, or a combination of both. A compensatory remapping of corticostriatal connectivity is constrained by existing anatomical connections and by the compensatory potential of the cortical region. In humans, the parietal cortex is anatomically connected to the dorsoposterior putamen but also to smaller portions of the ventroanterior putamen.[20] The inferior parietal cortex provides strong visual and somatosensory input to the ventral premotor cortex,[29] and in patients with PD, this ventral parieto-premotor circuit is hyperactivated during hand movements.[30] This may serve to compensate for impaired activity in medial motor circuits (such as the SMA) that are functionally connected to the posterior putamen.[31] The shift in corticostriatal connectivity of the inferior parietal cortex in *LRRK2* G2O19S mutation carriers also occurred within the parietal area where these same subjects showed increased task-related activity during a Stroop task.[9] The matched behavioral performance between *LRRK2* G2O19S mutation carriers and noncarriers in that study indicates that the increased task-related parietal activity is compensatory in nature. In symptomatic PD, the shift in corticostriatal connectivity was larger in the least affected hemisphere than in the most affected hemisphere.[5] Another study reported a shift in corticostriatal connectivity only in the right inferior parietal cortex, but most pronounced in patients with PD in whom the right hemisphere was less affected.[32] This supports the idea that the change in corticostriatal connectivity reflects a compensatory mechanism. The lack of lateralization in our current sample of asymptomatic *LRRK2* G2019S mutation carriers may be caused by the fact that we could not distinguish between most and least affected hemispheres, given the lack of clinical symptoms. Taken together, these findings suggest that *LRRK2* G2O19S mutation carriers shift their

computational resources to brain regions relatively unaffected by nigrostriatal dopamine depletion (i.e., the ventroanterior putamen), exploiting existing anatomical connections of this striatal region to cortical areas involved in motor control and cognition (i.e., the inferior parietal cortex).

The change in corticostriatal connectivity may also reflect pathologic changes occurring in the striatum. For instance, dopamine depletion in the basal ganglia is associated with a loss of segregation between parallel corticostriatal loops.[33] This may lead to functional crosstalk between different neural systems, with detrimental consequences. For example, it may lead to impaired sensorimotor integration, which has been found in healthy Parkin mutation carriers.[34] Furthermore, crosstalk between motor and cognitive corticostriatal loops may lead to impaired dual tasking, which is present both in patients with PD[35] and in healthy *LRRK2* G2O19S mutation carriers.[23]

Our voxel-based morphometry analysis suggests that the effects we report are unlikely caused by structural changes in *LRRK2* G2O19S mutation carriers. Other studies in different cohorts have reported a subtle increase in gray matter volume of the caudate[36] and parietal cuneus[37] of asymptomatic *LRRK2* mutation carriers, although the smaller sample size of these studies warrants caution. An important limitation of the current study is its cross-sectional nature. Future studies may longitudinally follow the cohort of *LRRK2* G2O19S mutation carriers reported here, testing how the shift in corticostriatal connectivity changes after subjects develop PD. In a similar vein, primate models of PD may test corticostriatal connectivity at different time points during progressive MPTP (1-methyl-4-phenyl-1,2,3,6-tetrahydropyridine) intoxication, in order to better outline the timing of compensatory mechanisms in a single cohort.[38]

We propose that the age-dependent shift in corticostriatal connectivity in healthy *LRRK2* G2019S mutation carriers is compensatory in nature. This provides a window of opportunity for implementing compensation-enhancing therapies. Such therapies may involve stimulation of compensatory brain areas using repetitive transcranial magnetic stimulation,[39] or behavioral training—for example, learning motor routines that involve the ventroanterior rather than the dorsoposterior putamen.[40]

AUTHOR CONTRIBUTIONS

Rick Helmich: analysis and interpretation of the data and drafting the manuscript. Avner Thaler: recruitment, clinical assessment, collection of the data, and revising the manuscript. Bart van Nuenen: interpretation of the data and revising the manuscript. Tanya Gurevich: clinical assessment and revision of the manuscript. Anat Mirelman: interpretation of the data and revising the manuscript. Karen Marder: design and conceptualization of the study, obtain funds, interpretation of data, revising the manuscript. Susan Bressman: design and conceptualization of the study, obtain funds, interpretation of data, revising the manuscript. Avi Orr-Urtreger: design and conceptualization of the study, obtain funds, genetic testing, revising the manuscript. Nir Giladi: design and conceptualization of the study, obtain funds, interpretation of data, revising the manuscript. Bas Bloem: design and conceptualization of the study, obtain funds, interpretation of data, revising the manuscript. Ivan Toni: design and conceptualization of the study, obtain funds, interpretation of data, revising the manuscript.

ACKNOWLEDGMENT

The authors thank the participants of this project for their invaluable participation and the staff of the AJ consortium for their contribution: Beth Israel Medical Center, New York, NY: Brooke Johannes. Tel Aviv Sourasky Medical Center, Israel: Maayan Zalis, DMD, Yaacov Balash, MD, Shabtai Hertzel, MD, Ziv Gan Or, PhD, Hila Kobo, MSc, Noa Bregman, MD, Meir Kestenbaum, MD, Talma Hendler, MD, PhD, Hedva Lehrman, MD, Einat Even Sapir, MD, PhD, Shiran Levy, Anat Shkedy, MD, and Michal Shtaigman, RN.

STUDY FUNDING

This work was supported by the Michael J. Fox Foundation for Parkinson Research and the Netherlands Organization for Scientific Research (VIDI grant 016.076.352 to B.R.B.).

DISCLOSURE

R. Helmich reports a grant from the Dutch Brain Foundation and the Van Leersum Foundation, outside the submitted work. A. Thaler and B. Van Nuenen report no disclosures relevant to the manuscript. T. Gurevich reports grants from Radboud University, grants from MJF Foundation, during the conduct of the study; grants from MJFF, grants from NPF, support from the pharmaceutical companies Teva, Novartis, AbbVie, and Medtronic, outside the submitted work. A. Mirelman reports no disclosures relevant to the manuscript. K. Marder reports grants from the Michael J. Fox Foundation, NIH grants NS036630, 1UL1RR024156, and Po412196, grants from U01NS052592, grants from Parkinson's Disease Foundation, grants from Huntington's Disease Foundation, and grants from CHDI, outside the submitted work. S. Bressman serves on the advisory boards of the Michael J. Fox Foundation, the Dystonia Medical Research Foundation, the Bachmann-Strauss Dystonia & Parkinson Foundation, and the board of We Move. She has consulted for Bristol-Myers Squibb. She has received research support from the Michael J. Fox Foundation, NIH, and Dystonia Medical Research Foundation. A. Orr-Urtreger reports no disclosures relevant to the manuscript. N. Giladi reports other from Teva Lundbeck, other from IntecPharma, other from NeuroDerm, other from Aramon Neuromedical Ltd., other from Pharma Two B, other from Novartis, other from UCB, other from MDS, grants from Michael J. Fox Foundation, grants from NPF, grants from EU 7th Framework, grants from ISF, and grants from Teva Innovative Ltd., outside the submitted work. B. Bloem reports grants from Netherlands Organization for Scientific Research, grants from Prinses Beatrix Foundation, grants from Stichting Internationaal Parkinson Fonds, grants from Alkemade-Keuls fonds, grants from Michael J. Fox Foundation, personal fees from Danone, personal fees from GlaxoSmithKline, personal fees from UCB, and personal fees from AbbVie, outside the submitted work. I. Toni reports no disclosures relevant to the manuscript. Go to Neurology.org for full disclosures.

Received May 28, 2014. Accepted in final form September 30, 2014.

REFERENCES

1. Kordower JH, Olanow CW, Dodiya HB, et al. Disease duration and the integrity of the nigrostriatal system in Parkinson's disease. Brain 2013;136:2419–2431.
2. Palop JJ, Chin J, Mucke L. A network dysfunction perspective on neurodegenerative diseases. Nature 2006;443:768–773.
3. Brück A, Aalto S, Nurmi E, Vahlberg T, Bergman J, Rinne JO. Striatal subregional 6-[18F]fluoro-L-dopa uptake in early Parkinson's disease: a two-year follow-up study. Mov Disord 2006;21:958–963.
4. Mounayar S, Boulet S, Tande D, et al. A new model to study compensatory mechanisms in MPTP-treated monkeys exhibiting recovery. Brain 2007;130:2898–2914.

5. Helmich RC, Derikx LC, Bakker M, Scheeringa R, Bloem BR, Toni I. Spatial remapping of cortico-striatal connectivity in Parkinson's disease. Cereb Cortex 2010; 20:1175–1186.
6. Poulopoulos M, Levy OA, Alcalay RN. The neuropathology of genetic Parkinson's disease. Mov Disord 2012;27: 831–842.
7. Healy DG, Falchi M, O'Sullivan SS, et al. Phenotype, genotype, and worldwide genetic penetrance of LRRK2-associated Parkinson's disease: a case-control study. Lancet Neurol 2008;7:583–590.
8. Mirelman A, Heman T, Yasinovsky K, et al. Fall risk and gait in Parkinson's disease: the role of the LRRK2 G2019S mutation. Mov Disord 2013;28:1683–1690.
9. Thaler A, Mirelman A, Helmich RC, et al. Neural correlates of executive functions in healthy G2019S LRRK2 mutation carriers. Cortex 2013;49:2501–2511.
10. van Nuenen BFL, Helmich RC, Ferraye M, et al. Cerebral pathological and compensatory mechanisms in the premotor phase of leucine-rich repeat kinase 2 parkinsonism. Brain 2012;135:3687–3698.
11. Hulihan MM, Ishihara-Paul L, Kachergus J, et al. LRRK2 Gly2019Ser penetrance in Arab-Berber patients from Tunisia: a case-control genetic study. Lancet Neurol 2008;7: 591–594.
12. Kachergus J, Mata IF, Hulihan M, et al. Identification of a novel LRRK2 mutation linked to autosomal dominant parkinsonism: evidence of a common founder across European populations. Am J Hum Genet 2005;76:672–680.
13. Marder K, Tang M, Alcalay R, et al. Age specific penetrance of the LRRK2 G2019S mutation in the Michael J. Fox Ashkenazi Jewish (AJ) LRRK2 Consortium. Neurology 2014;82(suppl):S17.002. Abstract.
14. Gan-Or Z, Giladi N, Rozovski U, et al. Genotype-phenotype correlations between GBA mutations and Parkinson disease risk and onset. Neurology 2008;70:2277–2283.
15. Fox MD, Raichle ME. Spontaneous fluctuations in brain activity observed with functional magnetic resonance imaging. Nat Rev Neurosci 2007;8:700–711.
16. Postuma RB, Dagher A. Basal ganglia functional connectivity based on a meta-analysis of 126 positron emission tomography and functional magnetic resonance imaging publications. Cereb Cortex 2005;16:1508–1521.
17. Lund TE, Nørgaard MD, Rostrup E, Rowe JB, Paulson OB. Motion or activity: their role in intra- and inter-subject variation in fMRI. NeuroImage 2005;26:960–964.
18. Friston KJ, Ashburner JT, Kiebel SJ, Nichols TE, Penny WD. Statistical Parametric Mapping: The Analysis of Functional Brain Images. Waltham, MA: Academic Press; 2011.
19. Alexander GE, DeLong MR, Strick PL. Parallel organization of functionally segregated circuits linking basal ganglia and cortex. Annu Rev Neurosci 1986;9:357–381.
20. Draganski B, Kherif F, Kloppel S, et al. Evidence for segregated and integrative connectivity patterns in the human basal ganglia. J Neurosci 2008;28:7143–7152.
21. Di Martino A, Scheres A, Margulies D, et al. Functional connectivity of human striatum: a resting state fMRI study. Cereb Cortex 2008;18:2735–2747.
22. Goldwurm S, Tunesi S, Tesei S, et al. Kin-cohort analysis of LRRK2-G2019S penetrance in Parkinson's disease. Mov Disord 2011;26:2144–2145.
23. Mirelman A, Gurevich T, Giladi N, Bar-Shira A, Orr-Urtreger A, Hausdorff JM. Gait alterations in healthy carriers of the LRRK2 G2019S mutation. Ann Neurol 2011; 69:193–197.
24. Thaler A, Mirelman A, Gurevich T, et al. Lower cognitive performance in healthy G2019S LRRK2 mutation carriers. Neurology 2012;79:1027–1032.
25. Sierra M, Sánchez-Juan P, Martínez-Rodríguez MI, et al. Olfaction and imaging biomarkers in premotor LRRK2 G2019S-associated Parkinson disease. Neurology 2013; 80:621–626.
26. Nandhagopal R, Mak E, Schulzer M, et al. Progression of dopaminergic dysfunction in a LRRK2 kindred: a multitracer PET study. Neurology 2008;71:1790–1795.
27. Adams JR, Van Netten H, Schulzer M, et al. PET in LRRK2 mutations: comparison to sporadic Parkinson's disease and evidence for presymptomatic compensation. Brain 2005;128:2777–2785.
28. Li X, Patel JC, Wang J, et al. Enhanced striatal dopamine transmission and motor performance with LRRK2 overexpression in mice is eliminated by familial Parkinson's disease mutation G2019S. J Neurosci 2010;30:1788–1797.
29. Gharbawie OA, Stepniewska I, Qi H, Kaas JH. Multiple parietal-frontal pathways mediate grasping in macaque monkeys. J Neurosci 2011;31:11660–11677.
30. Samuel M, Ceballos-Baumann AO, Blin J, et al. Evidence for lateral premotor and parietal overactivity in Parkinson's disease during sequential and bimanual movements: a PET study. Brain 1997;120:963–976.
31. Lehericy S, Ducros M, Krainik M, et al. 3-D diffusion tensor axonal tracking shows distinct SMA and pre-SMA projections to the human striatum. Cereb Cortex 2004;14: 1302–1309.
32. Hacker CD, Perlmutter JS, Criswell SR, Ances BM, Snyder AZ. Resting state functional connectivity of the striatum in Parkinson's disease. Brain 2012;135:3699–3711.
33. Bergman H, Feingold A, Nini A, et al. Physiological aspects of information processing in the basal ganglia of normal and parkinsonian primates. Trends Neurosci 1998;21:32–38.
34. Baumer T, Pramstaller PP, Siebner HR, et al. Sensorimotor integration is abnormal in asymptomatic Parkin mutation carriers: a TMS study. Neurology 2007;69:1976–1981.
35. Pessiglione M, Czernecki V, Pillon B, et al. An effect of dopamine depletion on decision-making: the temporal coupling of deliberation and execution. J Cogn Neurosci 2005;17:1886–1896.
36. Reetz K, Tadic V, Kasten M, et al. Structural imaging in the presymptomatic stage of genetically determined parkinsonism. Neurobiol Dis 2010;39:402–408.
37. Brockmann K, Gröger A, Di Santo A, et al. Clinical and brain imaging characteristics in leucine-rich repeat kinase 2-associated PD and asymptomatic mutation carriers. Mov Disord 2011;26:2335–2342.
38. Bezard E. Presymptomatic compensation in Parkinson's disease is not dopamine-mediated. Trends Neurosci 2003;26: 215–221.
39. van Nuenen BFL, Helmich RC, Buenen N, Van De Warrenburg BPC, Bloem BR, Toni I. Compensatory activity in the extrastriate body area of Parkinson's disease patients. J Neurosci 2012;32:9546–9553.
40. Cramer SC, Sur M, Dobkin BH, et al. Harnessing neuroplasticity for clinical applications. Brain 2011;134:1591–1609.